Effect of Carbonation on Microstructure of Cement Pastes with Different Water-to-Cement Ratios

K. Kopitha, S. Krishnya, Y. Elakneswaran, R. Kitagaki, Y. Yoda, M. Tsujino, and A. Nishida

Abstract The durability of the structures is the main concern in the field of engineering. Reinforcement corrosion is the most common cause of concrete structural deterioration. Corrosion of reinforcement results primarily from chloride ingress and carbonation. Cementitious materials are prone to carbonation as carbon dioxide is present everywhere in the atmosphere. For the durability prediction of cement-based materials, it is crucial to know the effect of carbonation on the microstructure of the cement matrix. This study examines how carbonation affects the microstructure of cement paste made up of Ordinary Portland Cement (OPC) with water-to-cement ratios (w/c) of 0.3, 0.4, and 0.5 with the help of the experiments and the newly developed model predicting the hydration products and porosity of the cement paste during the CO_2 gas diffusion. As part of this study, phenolphthalein was used to determine the carbonation depth. In addition to identifying the hydrated and carbonated products using X-Ray Diffraction (XRD) and Thermal Gravimetric Analysis (TGA), changes in microstructure were detected through Scanning Electron Microscope (SEM). Furthermore, the microstructures of cement paste samples that have been exposed to 5% carbon dioxide concentration for four months were compared. Carbonation products consist predominantly of calcite type polymorph of calcium carbonate, as revealed by XRD. Portlandite and C-S-H get carbonated simultaneously and the carbonation reaction increases with the increasing w/c in accordance with XRD and TGA results. Eventually, the experimental results of calcite and portlandite were compared with the predicted results from a newly developed COMSOL-IPHREEQC interface, and a better prediction of the numerical model was observed.

K. Kopitha (✉) · S. Krishnya · Y. Elakneswaran
Laboratory of Chemical Resources, Division of Sustainable Resources Engineering, Hokkaido University, Sapporo, Japan
e-mail: kopitha.kirushnapillai.n2@elms.hokudai.ac.jp

R. Kitagaki
Laboratory of Building Materials, Division of Architecture, Hokkaido University, Sapporo, Japan

Y. Yoda · M. Tsujino · A. Nishida
Center for Construction Engineering, Shimizu Corporation, Shimizu Institute of Technology, Tokyo, Japan

© The Author(s), under exclusive license to Springer Nature Singapore Pte Ltd. 2023

R. Dissanayake et al. (eds.), *ICSBE 2022*, Lecture Notes in Civil Engineering 362,
https://doi.org/10.1007/978-981-99-3471-3_11

Keywords Durability · Carbonation · Microstructure · COMSOL-IPHREEQC

1 Introduction

It is recognized that carbonation contributes significantly to corrosion in reinforced concrete [2]. The cement paste undergoes different chemical and mechanical changes during this physicochemical process, including microstructural and chemical changes in the cementitious matrix. As the pH of the pore solution decreases when concrete is carbonated, the passive layer formed on the reinforcement becomes unstable and leads to corrosion [3]. Therefore, it is important to study the factors affecting carbonation and hence durability of cementitious materials.

Hydrated cement consists of many phases that tend to carbonate. The carbonation rate is controlled by the amount of calcium-containing phases that are capable of dissolving and reacting to form calcite. Approximately 70–80% of hydrated cement's total solid volume consists of calcium silicate hydrates (C-S-H) and calcium hydroxide (CH) which can be carbonated easily [13]. A hydrated cement paste also consists of ettringite and monosulfoaluminate, which can be subjected to dissolution and subsequent carbonation due to pH drop by carbonation [9]. The degree of hydration that decides the amount of hydrated phases depends on the water-to-cement ratios (w/c) of the cement paste. The diffusion of CO_2 and the amount of hydration products in the cement matrix are the main factors that affect the carbonation rate [11]. W/c is one of the factors that determine the amount of hydration products. Hence, it is important to study the effect of w/c on both cement hydration and carbonation.

It has been found that the diffusion rate of CO_2 has the greatest influence on cement paste carbonation [3, 15]. Cement paste matrix pore structure and liquid saturation determine the diffusion rate of CO_2 and the w/c plays a very important role in cement paste porosity and pore size distribution [10]. It has been reported that the carbonation reaction decreases as the w/c is reduced [10]. It is important to investigate the effect of w/c on carbonation and hence to develop a numerical model based on that for better prediction of durability.

In recent years, researchers have become increasingly interested in simulating the realistic changes in the hydrated matrix during carbonation by integrating diffusion and reaction processes. It is noteworthy that the previously published work did not extensively consider the thermodynamic calculations for the carbonation of cement paste; instead, portlandite and C-S-H were only considered as hydration products and calcite as a carbonate phase [12, 14, 16]. Moreover, a gas phase within the cement matrix was neglected for CO_2 diffusion [12]. Hence, a new model platform is developed herein to address the limitations identified in previous models [7] and to predict the (i) diffusion of carbon dioxide gas and (ii) phase assemblage during transportation. To fully verify the feasibility of the newly developed model, further validation is recommended for the cement paste with different w/c and different CO_2 gas concentrations. The lack of experimental data available on the carbonation of

Table 1 Chemical composition of OPC using XRD and Bogue equation

Composition	XRD	Bogue equation
C_3S	60	51
C_2S	16	23
C_3A	07	10
C_4AF	12	09
Gypsum	04	

OPC paste samples with different w/c made this research team difficult to validate the newly developed COMSOL-IPHREEQC [6, 7] interface and to investigate the carbonation effects on the microstructure of cement paste sealed-cured with different w/c.

Therefore, this study is designed to evaluate the effect of w/c on the carbonation of hardened cement paste and its microstructural characteristics to validate the numerical model developed by this research group. For this study, w/c of 0.3,0.4, and 0.5 were selected. The hydrated cement paste was exposed to carbonation for four months and mineralogical assemblage was determined as a function of depth. In addition, scanning electron microscopy (SEM) was also used to identify microstructural changes. Finally, experimental data were compared with the predicted results of the numerical model (COMSOL-IPHREEQC interface).

2 Methodology

2.1 Materials

Ordinary Portland Cement (OPC), Class (H), confirmed to the Japan Industrial Standard JIS R 5201:2015, was used as the cementitious material. Blaine of the OPC used is 339 m^2/kg and the density is 3.16 g/cm^3. The chemical composition of cement is shown based on X-ray diffraction measurements and the Bogue equation is shown in Table 1.

2.2 Sample Preparation

Using a Hobart N50 5-Quart commercial stand mixer, mixing for three minutes was performed on cement paste samples with w/c values of 0.3, 0.4, and 0.5. Casting was done with cement paste mixtures in cylindrical moulds measuring 50 mm in diameter and 100 mm in height. Three samples were cast in each w/c to take the average of three samples in each measurement. After 24 h of casting, de-moulded samples were kept under sealed curing at 20 ± 2 °C for 28 days. After sealed curing, resin was

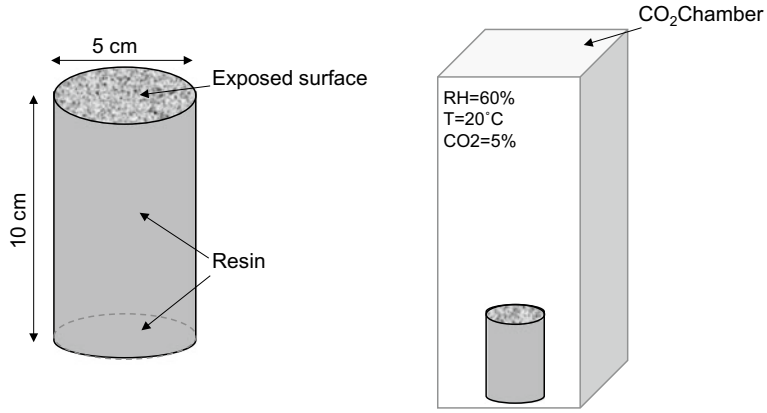

Fig. 1 Exposure of the samples to the CO_2

applied to all three faces except the bottom face of cylindrical samples and samples were exposed to carbon dioxide as shown in Fig. 1.

2.3 Exposure

The samples were exposed to CO_2 for four months in the CO_2 chamber where the concentration of CO_2 was at 5 ± 0.2%, the relative humidity at 60 ± 10%, and the temperature at 20 ± 2 °C. It was decided to use a relative humidity of 60% since this range produces the greatest carbonation rate [13]. Samples were kept in the chamber so that the face with no resin was upside. After the carbonation, samples were subjected to a phenolphthalein test, and then they were cut into discs of 2 mm as shown in Fig. 2.

2.4 Experimental Methods

2.4.1 Phenolphthalein Test

After four months of carbonation, samples were taken out from the CO_2 chamber and those cylindrical samples were split. The carbonation depth of carbonated samples was determined using phenolphthalein spray (0.4 g/L Phenolphthalein in 40 vol% ethanol). Three measurements were made of the colourless region over three samples and the average was recorded for each w/c.

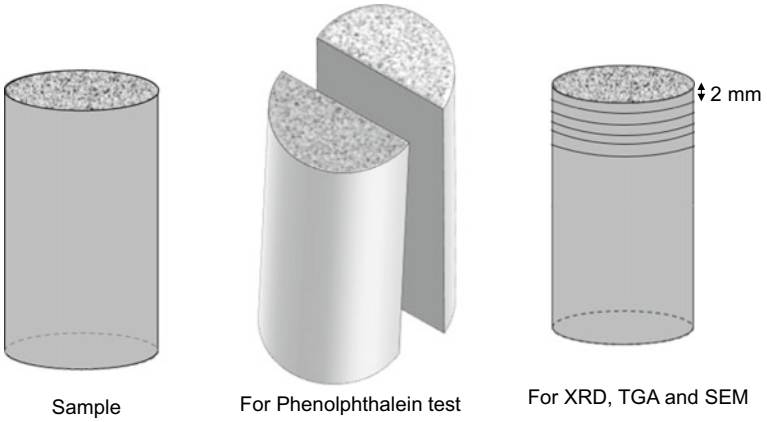

Fig. 2 Position of the cutting of samples for subsequent analysis

2.4.2 X-Ray Diffraction (XRD) Analysis

A Rigaku X-ray diffractometer with CuKα radiation was used to measure the crystalline phases in the samples of carbonated cement paste. A range of 5–70° 2θ was scanned with a step size of 0.02° and a rotating speed of 6.5°/min. Grinding the discs resulted in powder samples that were measured after four months of carbonation. For the quantitative analysis of XRD patterns, the Profex/BGMN software package was used [4]. This program permits the estimation of the weight fractions of crystalline phases using the Rietveld refinement procedure. The internal standard method was applied to obtain the absolute mass fractions of the crystalline phases. The sample was mixed with 10 wt% corundum as an internal standard.

2.4.3 Thermogravimetric Analysis (TGA)

TGA was carried out under nitrogen with a flow rate of 200 mL/min on powdered samples with a HITACHI TG/DTA 7220 and a heating rate of 10 °C/min from 20 to 950 °C. At the temperature range 400–500 °C and 540–950 °C, weight loss was used to quantify the $Ca(OH)_2$ and $CaCO_3$ respectively. The amount of $Ca(OH)_2$ and $CaCO_3$ present in the carbonated samples were calculated according to the following Eqs. (1) and (2) [1, 11, 17].

$$\%Ca(OH)_2 = \frac{(M_{400\,^\circ C} - M_{500\,^\circ C})}{M_{\text{Sample}}} \times \frac{74.09}{18.01} \times 100 \tag{1}$$

$$\%CaCO_3 = \frac{(M_{540\,^\circ C} - M_{950\,^\circ C})}{M_{\text{Sample}}} \times \frac{100.09}{44.01} \times 100 \tag{2}$$

At a given temperature, the sample mass is M. The TGA tests were performed with 15 mg (±0.2 mg) of powder derived from disc samples.

2.4.4 Scanning Electron Microscopy (SEM)

Backscattered electrons (BSE) images were obtained using SEM. BSE images can be used for phase identification based on the grey levels. Before SEM analysis, epoxy-impregnated samples were polished and coated with gold. A 15 kV accelerating voltage and 10 mm working distance were set for this analysis.

2.4.5 Thermodynamic Modelling

A new reactive transport model including the cement hydration model, thermodynamic calculation (including the kinetic model for C-S-H dissolution) and species transportation calculation is herein proposed to predict hydration products and porosity of the cement paste during the carbon dioxide gas diffusion. The elementary characteristics to determine the formation of hardened cement matrix during the hydration period such as chemical and physical properties of cement, mixture recipe and boundary conditions are the input parameters for the hydration model while the ionic concentration in the exposed environment, initiation of transport reaction relative to hydration time and duration of the transport reaction are the compulsory input data for the transport model. The cement hydration model is used to compute the dissolution rate of each clinker mineral as a function of time. Thermodynamic calculations are performed using PHREEQC open-source package and COMSOL Multiphysics is used for the transportation calculations. The implemented approach used to predict the hydration products and transport properties are detailed in our previous work [6–8]. This modelling platform is developed in MATLAB language and LiveLink™ for MATLAB® is used for data transference between MATLAB and COMSOL Multiphysics.

3 Results and Discussion

3.1 Phenolphthalein Test

Phenolphthalein-sprayed images of carbonated samples are shown in Fig. 3. The samples having w/c of 0.3 exhibited the lowest carbonation depth of 0.5 mm. This could be due to a dense microstructure that prevents CO_2 from diffusing for carbonation. The carbonation depth of samples having w/c of 0.4 and 0.5 exhibited carbonation depth of 1 mm and 4 mm respectively.

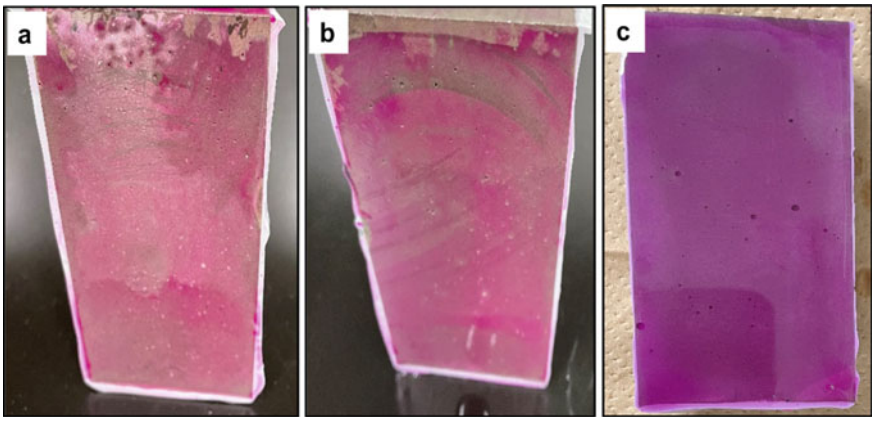

Fig. 3 Phenolphthalein-sprayed images of carbonated samples (**a**: w/c = 0.5, **b**: w/c = 0.4, **c**: w/c = 0.3)

3.2 XRD

The first layers from the surface exposed to carbonation (0–2 mm) of cement paste samples were subjected to XRD. Plots of the XRD pattern of carbonated samples having different w/c are shown in Fig. 4. Carbonated samples mainly contained calcium hydroxide and calcite. Calcite-type calcium carbonate was found to be the main carbonation product based on XRD results. Figure 5 illustrates the Rietveld quantitative analysis of the XRD scan. All non-crystalline phases such as C-S-H and silica gel belong to the amorphous part. The polymorphs of calcium carbonate such as vaterite, aragonite and calcite were described with a cumulative term called calcium carbonate. According to the results, there was simultaneous carbonation of portlandite and C-S-H. As a thermodynamic principle, it is imperative that all portlandite carbonates before C-S-H, but that is not the case in practice. Carbonated product was high in samples having w/c of 0.5. Studies [2, 5, 15] have consistently shown this result, whereby the amount of hydrated phases is high in the samples having high w/c and it enhances the rate of carbonation reaction. Figure 5 shows that amount of amorphous content in samples with w/c of 0.5 is less than that of w/c of 0.4. This is mainly due to the carbonation of amorphous phases such as C-S-H carbonated more in the samples with w/c of 0.5 as they have more diffusion rate of CO_2.

3.3 TGA

The first layers from the surface exposed to carbonation (0–2 mm) of cement paste samples were subjected to TGA. Figure 6 compares the weight loss (TG) and the

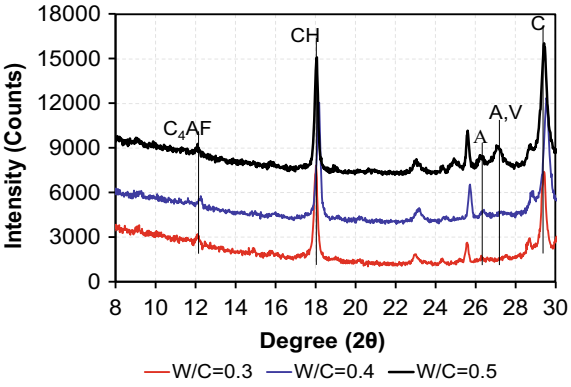

Fig. 4 XRD plots of carbonated samples having different w/c (CH: calcium hydroxide, A: aragonite, V: vaterite, C: calcite)

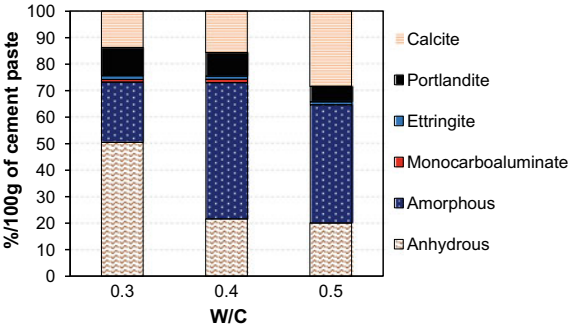

Fig. 5 Rietveld quantitative analysis of the XRD scan of carbonated samples having different w/c

differential thermal (DTG) curves of samples with varying w/c. C-S-H, Aft, and AFm phases are decomposed at temperatures of 30–300 °C, causing mass loss. From the XRD analysis, AFt and AFm phases were of small amount. Therefore, the decomposition peak corresponding to this temperature range was mainly due to the decomposition of C-S-H.

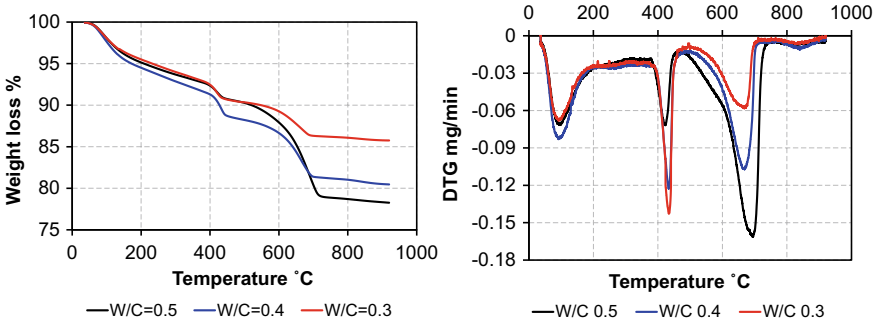

Fig. 6 TGA curves of carbonated samples having different w/c

From the DTG curve, it can be noticed that the decomposition peak of the sample with w/c of 0.5 shows a small peak compared to the sample with w/c of 0.4 in the temperature range of 30–300 °C. It shows that the amount of C-S-H is less as observed in the XRD result (Fig. 5) and confirms the carbonation of C-S-H. The samples having w/c of 0.3 shows a smaller decomposition peak in the specific temperature range compared to the other two samples as it has a low degree of hydration due to low water content.

$Ca(OH)_2$ decomposes at 400–500 °C, which results in weight loss. When the w/c was increased, the $Ca(OH)_2$ decreased significantly, mainly because $Ca(OH)_2$ was converted to $CaCO_3$. $CaCO_3$ decomposes in the temperature range of 540–950 °C. $CaCO_3$ content was higher in samples with w/c of 0.5, primarily due to active hydration products being converted to $CaCO_3$.

3.4 SEM

The first layers from the surface exposed to carbonation (0–2 mm) of cement paste samples were subjected to SEM. Figure 7 shows the BSE images of the samples having different w/c. The brightest region in the BSE image represents anhydrous cement, and black represents pores. Figure 7a depicts a sample with w/c of 0.5, with brighter products corresponding to polymorphs of $CaCO_3$ precipitated during carbonation mixed with decalcified C-S-H or silica gel appearing in the majority of areas compared to Fig. 7b, c. In contrast, Fig. 7b, c show that the samples having less w/c having the light grey products correspond to $Ca(OH)_2$ and C-S-H in the most region.

3.5 Thermodynamic Modelling

To verify the predictability of the proposed model on carbon dioxide diffusion, the computed results of the weight percentage of calcite and portlandite are compared with the XRD experimental results for the cement paste of w/c 0.4 after four months of exposure in the environment of 5% (of the air volume) CO_2 concentration. The first five layers from the surface exposed to carbonation (0–10 mm) of cement paste samples were subjected to XRD. The predicted results from the coupled model for calcite and portlandite weight percentages show an excellent agreement with experimental results as shown in Fig. 8. During the carbonation process, portlandite dissolves due to the decrease of pH, which leads to the reduction of portlandite weight percentage in the cement matrix as depicted in Fig. 8 and forms as calcite.

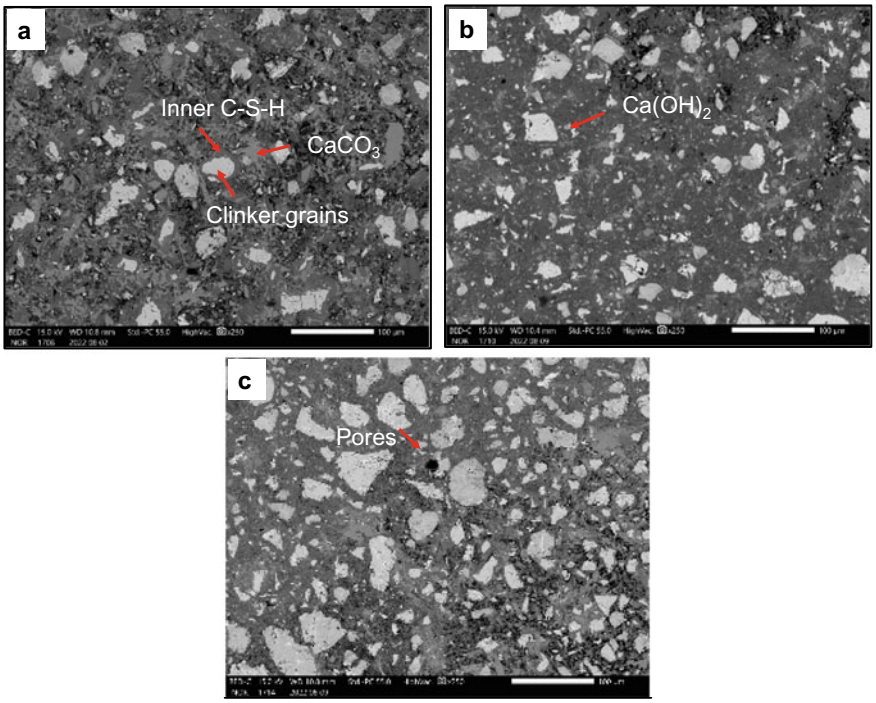

Fig. 7 BSE images of carbonated samples having different w/c (**a**: w/c = 0.5, **b**: w/c = 0.4, **c**: w/c = 0.3)

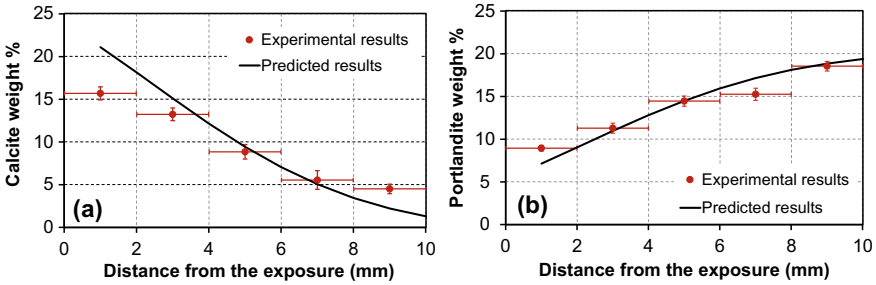

Fig. 8 Comparison of predicted calcite and portlandite weight % with experimental results

4 Conclusions

The influence of w/c of cement paste on carbonation and thus microstructural properties were studied and the results were compared with the numerical model that has been developed using the COMSOL-IPHREEQC interface. XRD, TG and SEM were

used to analyse the effect of w/c on carbonation and the changes in the microstructure due to carbonation. Based on the findings, the following conclusions can be drawn:

1. XRD results revealed that calcite-type calcium carbonate was found to be the main carbonation product.
2. From the XRD and TG results, there was simultaneous carbonation of portlandite and C-S-H.
3. Based on the phenolphthalein test, XRD, TG, and SEM analysis, carbonation increases with increasing w/c.
4. The predicted results from the coupled model for calcite and portlandite weight percentages show an excellent agreement with experimental results.

References

1. Ashraf W, Olek J (2016) Carbonation behavior of hydraulic and non-hydraulic calcium silicates: potential of utilizing low-lime calcium silicates in cement-based materials. J Mater Sci 51(13):6173–6191
2. Boumaaza M et al (2020) Influence of carbonation on the microstructure and the gas diffusivity of hardened cement pastes. Constr Build Mater 253
3. Castellote M et al (2009) Chemical changes and phase analysis of OPC pastes carbonated at different CO_2 concentrations. Mater Struct/Mater Constr 42(4):515–525
4. Doebelin N, Kleeberg R (2015) Profex: a graphical user interface for the Rietveld refinement program BGMN. J Appl Cryst
5. Kim YY et al (2014) Effect of W/C ratio on durability and porosity in cement mortar with constant cement amount. Adv Mater Sci Eng 2014
6. Krishnya S et al (2022) Coupled multi-ionic transport model with hydration model for the chloride ion ingression in cement paste. JCI 44(1):514–519. Available at: JCI
7. Krishnya S, Kopitha K et al (2022) Coupling CO_2 (g) diffusion and geochemistry for the carbonation of cement paste. In: 76th RILEM annual week 2022, pp 1–4
8. Krishnya S, Yoda Y, Elakneswaran Y (2021) A two-stage model for the prediction of mechanical properties of cement paste. Cem Concr Compos 115
9. Lagerblad B (2005) Carbon dioxide uptake during concrete life cycle: state of the art. Swedish Cement and Concrete Research Institute
10. Lo TY, Tang WC, Nadeem A (2008) Comparison of carbonation of lightweight concrete with normal weight concrete at similar strength levels. Constr Build Mater 22(8):1648–1655
11. Mehdizadeh H et al (2021) Effect of water-to-cement ratio induced hydration on the accelerated carbonation of cement pastes. Environ Pollut 280
12. Phung QT et al (2016) 'Modelling the carbonation of cement pastes under a CO_2 pressure gradient considering both diffusive and convective transport. Constr Build Mater 114:333–351
13. Shah V et al (2018) Changes in microstructure characteristics of cement paste on carbonation. Cem Concr Res 109:184–197
14. Shen X et al (2019) Numerical study of carbonation and its effect on chloride binding in concrete. Cem Concr Compos 104(September 2018):103–402
15. Wang J et al (2019) Accelerated carbonation of hardened cement pastes: influence of porosity. Constr Build Mater 225:159–169
16. Xie M, Dangla P, Li K (2021) 'Reactive transport modelling of concurrent chloride ingress and carbonation in concrete. Mater Struct/Mater Constr 54(5):1–19
17. Zajac M et al (2020) Phase assemblage and microstructure of cement paste subjected to enforced, wet carbonation. Cem Concr Res 130